# Insights into the Photoelectron Spectroscopy of Chlorofluoroethenes Studied by Density-Functional and Coupled-Cluster Theories

Cyong-Huei Huang, Shang-Yi Chou, Shiu-Bau Jang, Yu-Chieh Lin, Chien-En Li, Chiing-Chang Chen, and Jia-Lin Chang*

Department of Science Education and Application, National Taichung University of Education, Taichung 40306, Taiwan, Republic of China

S *Supporting Information*

ABSTRACT: The first two ionic states of chlorofluoroethenes were studied by using both time-independent and time-dependent density-functional theories. We calculated the equilibrium geometries and harmonic vibrational frequencies of 1,1-, *cis*-, and *trans*-C_2H_2FCl and their cations by using the B3LYP and B3PW91 functionals together with the cc-pVTZ and aug-cc-pVTZ basis sets. Franck–Condon factors were computed by the method developed in our group, in which the Duschinsky effect was treated explicitly. A new technique, named alignment transformation, followed by Euler transformations was developed to achieve the Eckart conditions. The adiabatic ionization energies were calculated by the CCSD(T) method extrapolated to the complete basis set limit. Insights into the simulated photoelectron spectra of C_2H_2FCl indicate that the resolutions of recent threshold photoelectron experiments are not high enough to detect individual transitions. The high-resolution photoelectron spectra of C_2H_2FCl are predicted for future reference. The computed adiabatic ionization energies of the three isomers of C_2H_2FCl are in accord with the experiments with the absolute deviations ranging from 0.004 to 0.021 eV. We suggest that the agreement between experimental and theoretical spectra should be a key criterion to judge whether a spectral assignment is reasonable.
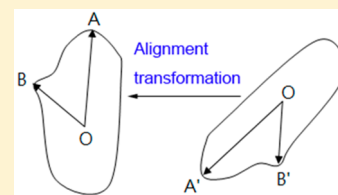
INTRODUCTION

We have recently developed an analytical approach for computing Franck–Condon integrals of harmonic oscillators with arbitrary dimensions,[1–5] in which the mode-mixing Duschinsky effect[6] is treated explicitly. Our approach is useful to interpret or predict vibronic spectra of molecules and is an alternative to other compatible techniques.[7–16] In this work, we applied our approach to study the photoelectron spectra of the three isomers of chlorofluoroethenes, i.e., 1,1-, *cis*-, and *trans*-C_2H_2FCl.

Halogenated ethenes are air pollutants and thus are important in environmental transformation processes, such as the generation of halogen atoms from photolysis and its subsequent chemical reactions with ozone and hydroxyl radicals in the atmosphere.[17,18] The lower-resolution photoelectron spectra of halogenated ethenes have been recorded for a long time,[19–22] but recent higher-resolution studies provide new insights into their vibronic structures and equilibrium geometries. For example, Harvey et al. recorded the valence threshold photoelectron spectra of four fluorinated ethenes (C_2H_3F, 1,1-$C_2H_2F_2$, C_2HF_3, and C_2F_4).[23] With the aid of density-functional theory computations and Franck–Condon simulations they reassigned some vibrational modes present in the spectra. In addition, the equilibrium structure of the ground electronic state of 1,1-$C_2H_2F_2^+$ was inferred to be no longer planar. They show that ab initio vibrational frequencies together with the observed vibrational spacings do not always suffice to assign a vibronic spectrum. We agree with them and claim in a previous publication that the best marriage of

quantum theory and experimental spectroscopy should be that both the calculated energy and intensity distribution are closely matched with experiments.[4]

In 2014, Locht et al. reported the threshold photoelectron spectra of the three isomers of C_2H_2FCl and analyzed their vibrational structures according to ab initio calculations of equilibrium geometries and vibrational frequencies.[24,25] Although some other theoretical studies on C_2H_2FCl exist in the literature,[26–33] the lack of information about theoretical intensity distributions motivated us to carry out the present study, in which different computational approaches of density-functional and coupled-cluster theories were adopted for comparison. We show in this report that the simulated photoelectron spectra of C_2H_2FCl provide detailed insights into the vibrational structures. Most importantly, the theoretical spectra indicate that the resolutions of the previous experiments[24,25] are not high enough to identify individual transitions. Most observed bands contain several transition signals and their shapes are consequences of overlapped peaks. Accordingly, the reported experimental vibrational frequencies and anharmonic constants[24,25] need to be verified by advanced experiments.

In this article, we also present a new technique by which the Eckart conditions[34,35] can be achieved. The Eckart conditions minimize the mixing of rotational and vibrational modes in two

molecular states with different geometries, which is important for simulating the vibronic spectrum of molecules, as well as in studying the transition state of chemical reaction.[36] We designed an alignment transformation technique followed by Euler transformations to fulfill the desired requirements.

The rest of this article is organized as follows. The next section describes the theoretical methods, including the quantum-chemistry computations, the proposed alignment transformation technique, and our Euler transformation formulas. The following section presents the results of computation for the equilibrium geometries, vibrational frequencies, photoelectron spectra, and adiabatic ionization energies. The significance of the present study in interpreting and predicting the photoelectron spectra of the three isomers of C_2H_2FCl is discussed. Finally, the Conclusions section draws concluding remarks of this work.

■ THEORETICAL METHODS

Quantum-Chemistry Computations. The optimized geometries and harmonic vibrational frequencies of 1,1-, *cis*-, and *trans*-C_2H_2FCl, as well as their first two cationic states were obtained by using the density-functional theory (B3LYP and B3PW91 functionals) combined with the basis sets cc-pVTZ and aug-cc-pVTZ (VTZ and AVTZ hereafter). The time-dependent B3LYP and B3PW91 methods were also adopted to compute the first excited state of the three isomers of C_2H_2FCl. Similar computations were also performed by using the coupled-cluster singles and doubles (CCSD) and equation-of-motion CCSD (EOM-CCSD) methods with the 6-311+G(d), cc-pVDZ, and cc-pVTZ basis sets. However, except for *trans*-$C_2H_2FCl^+(\tilde{A}^2A')$, the simulated spectra are less satisfactory and we just show their results with brief discussions in the Supporting Information for completeness.

Franck−Condon factors were calculated by using the approach developed in this group, which has been described in detail elsewhere.[5] The photoelectron spectra were simulated by taking the FCFs as peak heights and the Gaussian function as the line shape. In our simulation, the full width at the half-maximum (fwhm) of the peaks was set to 10 cm^{-1} for predicting high-resolution spectra, whereas it was adjusted until a good match was achieved when the simulated spectrum was copmared with the experiment.

The adiabatic ionization energies (AIEs) were computed by using the approach developed by Peterson et al., in which the CCSD(T) energies were extrapolated to the complete basis set (CBS) limit with aug-cc-pVXZ (X = D, T, Q, 5) according to the following formula,[37]

$$E(n) = E_{CBS} + A\exp(-(n-1)) + B\exp(-(n-1)^2) \tag{1}$$

where $E(n)$ is the energy of the nth level (n = 2−5 for X = D−5), E_{CBS} is the asymptotic CBS limit energy, and A and B are adjusting parameters. In the AIE computation, the equilibrium structures and zero-point energy corrections were both taken from the B3LYP/AVTZ calculations. All of the quantum-chemistry calculations were performed by utilizing the Gaussian 09 package.[38]

Alignment Transformation and Euler Transformation. Before computing FCFs, one needs to obtain the geometrical displacements **D** between two electronic states, which can be calculated by[2]

$$\mathbf{D} = \mathbf{L}'\mathbf{M}^{1/2}(\mathbf{X}_0 - \mathbf{X}'_0) \tag{2}$$

where $\mathbf{L}'$ is the displace matrix of normal modes of the initial state, $\mathbf{M}$ is a diagonal matrix consisting of atomic masses, and $\mathbf{X}_0$ and $\mathbf{X}'_0$ are the Cartesian coordinates of equilibrium structures of the final and the initial states, respectively. Occasionally, we encounter cases where the definitions of coordinate systems ($\mathbf{X}_0$ and $\mathbf{X}'_0$) are different for two electronic states when the Gaussian 09 package is used. It is likely that the change in molecular structures leads to the application of different rules of the standard orientation adopted by Gaussian 09. For example, the atomic positions of 1,1-$C_2H_2FCl(\tilde{X}^1A')$ and 1,1-$C_2H_2FCl^+(\tilde{A}^2A')$ returned by Gaussian 09 are shown in Figure 1a,b, respectively. The CH_2 group is located in the
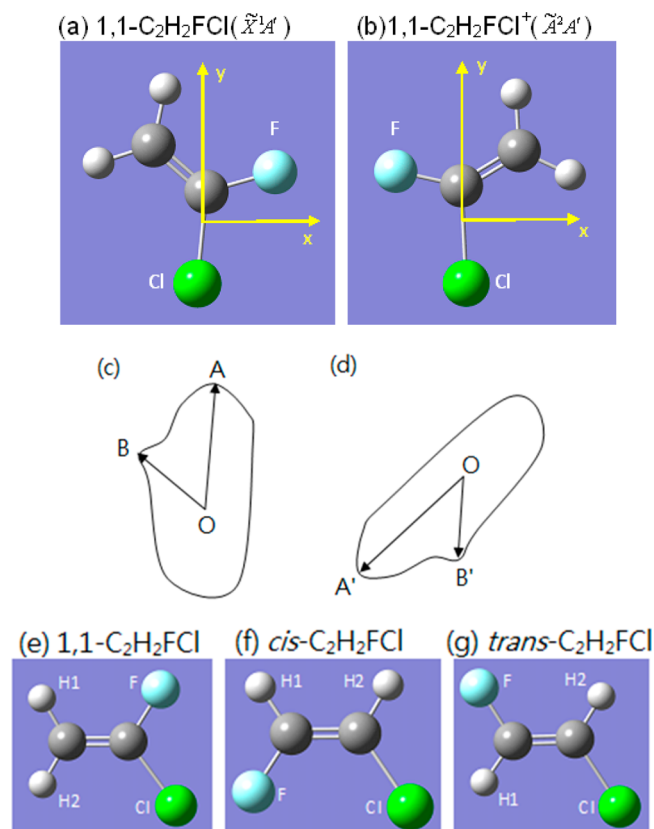

Figure 1. Atomic positions of (a) 1,1-$C_2H_2FCl(\tilde{X}^1A')$ and (b) 1,1-$C_2H_2FCl^+(\tilde{A}^2A')$ returned by Gaussian 09. A schematic diagram showing (c) a molecular structure that is differently oriented with (d) the structure of another electronic state, where O is the coordinate origin (center of mass), A is the furthermost atom from O, and B is the furthermost atom from the OA line. The arrangement of atoms for (e) 1,1-C_2H_2FCl, (f) *cis*-C_2H_2FCl, and (g) *trans*-C_2H_2FCl.

second quadrant of the *xy*-plane for 1,1-$C_2H_2FCl(\tilde{X}^1A')$, whereas it is in the first quadrant for 1,1-$C_2H_2FCl^+(\tilde{A}^2A')$. The two choices are alternative and do not cause any problem in the computation of molecular properties. Nevertheless, one will obtain an erroneous conclusion that the geometrical change is drastic, if the coordinate difference is computed from ($\mathbf{X}_0 - \mathbf{X}'_0$) directly.

To get the accurate geometrical change, the coordinates of one electronic state should be transformed such that they are close to those of the other state and to satisfy the Eckart conditions.[34,35] This is usually done by Euler transformation or by quaternion rotation.[9−11] In this work, we develop a new

technique, named alignment transformation, followed by Euler transformations to accomplish the task.

The key idea of alignment transformation is to align two structures of a molecule such that atoms in one structure are located close to their positions in the other state. We choose two atoms as the characteristic points to achieve the alignment. Atom A is the furthermost atom from the origin O located at the center of mass, and B is the atom furthermost from the OA line (Figure 1c). The corresponding positions are denoted as A′ and B′ in the other state (Figure 1d). The center of mass of both states coincides at O. The alignment transformation is accomplished by two steps. First, the molecule is rotated around $\mathbf{n}_1 = \mathbf{OA'} \times \mathbf{OA}$ such that $\mathbf{OA'}$ is along $\mathbf{OA}$. Then, it is rotated around $\mathbf{OA'}$ such that $\mathbf{n}_2 = \mathbf{OA'} \times \mathbf{OB'}$ is along $\mathbf{n}_3 = \mathbf{OA} \times \mathbf{OB}$. With such transformations, the AOB and A′OB′ planes coincide and the corresponding atoms in two molecular states are positioned in the proximity, which speeds up the convergence of the subsequent Euler transformations.

Our formulas of Euler transformations are derived in the Appendix. The primary equations are

$$\left[\sum m(y_0 y + z_0 z)\right] s_1 + \left(-\sum m y_0 x\right) s_2 + \left(-\sum m z_0 x\right) s_3$$
$$= \sum m(z_0 y - y_0 z)$$

$$\left(-\sum m x_0 y\right) s_1 + \left[\sum m(z_0 z + x_0 x)\right] s_2 + \left(-\sum m z_0 y\right) s_3$$
$$= \sum m(x_0 z - z_0 x)$$

$$\left(-\sum m x_0 z\right) s_1 + \left(-\sum m y_0 z\right) s_2 + \left[\sum m(x_0 x + y_0 y)\right] s_3$$
$$= \sum m(y_0 x - x_0 y)$$

(3)

or in a matrix form

$$\begin{pmatrix} a_{11} & a_{12} & a_{13} \\ a_{21} & a_{22} & a_{23} \\ a_{31} & a_{32} & a_{33} \end{pmatrix} \begin{pmatrix} s_1 \\ s_2 \\ s_3 \end{pmatrix} = \begin{pmatrix} b_1 \\ b_2 \\ b_3 \end{pmatrix}$$

(4)

Our derivation is similar to that done by Chen[39] but with two differences. One is that we rotate the molecule counterclockwise around the three Cartesian axes, whereas Chen rotated the molecule counterclockwise around the x and z axes but clockwise around y.[39] The other is that we use a tighter approximation condition (see Appendix).

Due to different approximations, our formulas (eqs 3 and 4) are slightly different from those derived by Chen.[39] In our formulas, the coefficient matrix elements in eq 4 are all different, whereas Chen's matrix is symmetric, i.e., $a_{ij} = a_{ji}$. We have tested the procedures of alignment transformation followed by Euler transformations and also compared the efficiency between our and Chen's approaches. Without alignment transformation, the direct application of Euler transformation is less efficient and sometimes goes to wrong positions. In contrast, the alignment transformation speeds up the convergence of Euler transformation and always leads to the correct positions. Moreover, our approach is usually faster than Chen's[39] by one or two iteration cycles.

■ RESULTS AND DISCUSSION

Equilibrium Geometries. The equilibrium geometries of 1,1-, cis-, and trans-C_2H_2FCl and their cationic states are listed in Tables 1−3, respectively, and the arrangement of atoms is shown in Figure 1e−g. Only the B3LYP/AVTZ results are

Table 1. Equilibrium Geometries of 1,1-C_2H_2FCl and Its Cations[a]

parameter[b]	X		X+	A+	
	B3LYP	expt[c]	B3LYP	B3LYP	TD-B3LYP
R_{CC}	131.80	132.67	140.25	129.87	131.38
R_{CH1}	107.93	108.03	108.36	108.89	108.47
R_{CH2}	107.64	108.19	108.09	108.32	108.01
R_{CF}	133.52	134.12	128.32	129.01	129.10
R_{CCl}	172.86	170.42	165.39	187.49	182.92
A_{CCH1}	119.5	119.2	119.1	118.2	118.0
A_{CCH2}	120.6	119.4	120.1	123.3	122.6
A_{CCF}	122.7	121.8	119.2	136.1	131.2
A_{CCCl}	125.8	126.3	123.8	118.6	123.4

[a]X stands for the neutral ground state, X+ for the cationic ground state, and A+ for the first excited state of cation. The calculation basis set is aug-cc-pVTZ. [b]R stands for bond lengths (in pm) and A for bond angles (in deg). [c]Experimental values are taken from ref 40.

Table 2. Equilibrium Geometries of cis-C_2H_2FCl and Its Cations[a]

parameter[b]	X		X+	A+	
	B3LYP	expt[c]	B3LYP	B3LYP	TD-B3LYP
R_{CC}	132.15	133.0	139.89	132.84	133.17
R_{CH1}	108.05	108.1	108.65	108.42	108.33
R_{CH2}	107.74	107.7	108.34	109.41	108.66
R_{CF}	133.79	132.7	127.80	130.90	130.65
R_{CCl}	172.96	171.5	164.88	173.75	175.54
A_{CCH1}	123.3	123.8	123.1	121.3	122.0
A_{CCH2}	120.6	121.9	119.5	126.1	126.2
A_{CCF}	123.2	122.8	120.8	122.4	121.7
A_{CCCl}	123.9	123.1	122.2	123.6	122.5

[a]X stands for the neutral ground state, X+ for the cationic ground state, and A+ for the first excited state of cation. The calculation basis set is aug-cc-pVTZ. [b]R stands for bond lengths (in pm) and A for bond angles (in deg). [c]Experimental values are taken from ref 29.

Table 3. Equilibrium Geometries of trans-C_2H_2FCl and Its Cations[a]

parameter[b]	X		X+	A+	
	B3LYP	calc[c]	B3LYP	B3LYP	TD-B3LYP
R_{CC}	132.01	132.4	139.54	133.31	133.42
R_{CH1}	107.97	107.9	108.64	108.64	108.23
R_{CH2}	107.84	107.8	108.48	110.47	109.18
R_{CF}	134.60	133.8	127.99	130.22	130.36
R_{CCl}	173.52	172.0	165.11	170.74	174.42
A_{CCH1}	126.2	125.6	125.2	124.7	126.5
A_{CCH2}	123.2	123.1	121.3	123.3	125.5
A_{CCF}	120.4	120.3	118.5	120.1	118.4
A_{CCCl}	121.4	120.6	120.0	127.9	124.8

[a]X stands for the neutral ground state, X+ for the cationic ground state, and A+ for the first excited state of cation. The calculation basis set is aug-cc-pVTZ. [b]R stands for bond lengths (in pm) and A for bond angles (in deg). [c]The "empirical" structure is calculated by using the CCSD(T) method.[30]

shown for simplicity because they agree with experiments well and also because switching to the B3PW91 method or the VTZ basis set did not result in significant deviations. The B3PW91/AVTZ results are given in the Supporting Information. For 1,1-C_2H_2FCl, the deviations of bond lengths R_{CC}, R_{CF}, and R_{CCl}

compared with the experimental values[40] are −0.87, −0.60, and +2.44 pm (Table 1), respectively, which are comparable to the corresponding deviations 1.07, 0.86, and 2.82 pm of the CCSD(FC)/AVDZ method performed by Locht et al.[24] The bond angles calculated by B3LYP/AVTZ are different from the experimental values by 0.3 to 1.2° (Table 1).[40]

For cis-C_2H_2FCl, the B3LYP/AVTZ results of R_{CC}, R_{CF}, and R_{CCl} are deviated from the experiment by −0.85, +1.09, and +1.46 pm, respectively, and the difference of bond angles between theory and experiment ranges from 0.5° to 1.3° (Table 2).[29] There is no experimental structure of trans-C_2H_2FCl for comparison. Comparing with the "empirical" structure calculated by using the CCSD(T) method,[30] we get the small deviations of −0.39, +0.8, and +1.52 pm for R_{CC}, R_{CF}, and R_{CCl}, respectively, and the agreement of bond angles is within 0.8° (Table 3). In addition, for both cis- and trans-C_2H_2FCl, our computational results (Tables 2 and 3) are in accord with the CCSD(T)/cc-pV∞Z results and the recommended ab initio equilibrium geometries reported by Puzzarini et al.[28−31]

The changes of equilibrium geometries of cationic C_2H_2FCl with respect to the neutral are useful in interpreting the vibrational structures of photoelectron spectra, as discussed in the Photoelectron Spectra section.

Vibrational Frequencies. The harmonic vibrational frequencies of the three isomers of C_2H_2FCl are listed in Tables 4−6. C_2H_2FCl belongs to the C_s point group and the

Table 4. Harmonic Vibrational Frequencies (in cm^{-1}) of 1,1-C_2H_2FCl and Its Cations[a]

mode	X		X+	A+	
	B3LYP	expt[b]	B3LYP	B3LYP	TD-B3LYP
ν_1	3280	3070	3268	3195	3249
ν_2	3179	3020	3145	3081	3138
ν_3	1708	1656	1498	1782	1788
ν_4	1408	1385	1415	1363	1406
ν_5	1180	1188	1294	1075	1165
ν_6	955	947	999	914	953
ν_7	688	700	747	473	588
ν_8	432	433	456	324	373
ν_9	371	370	367	181	257
ν_{10}	869	835	949	894	934
ν_{11}	721	610	367[c]	728	707
ν_{12}	534	514	563	465	496

[a]X stands for the neutral ground state, X+ for the cationic ground state, and A+ for the first excited state of cation. The calculation basis set is aug-cc-pVTZ. [b]Experimental values are taken from ref 40. [c]The underlines denote normal modes whose orders are changed in comparison to those of the ground state.

symmetry species are a′ for $\nu_1 \sim \nu_9$ and a″ for $\nu_{10} \sim \nu_{12}$. For the neutral ground state, the computed frequencies are in agreement with experiment and, on average, are 3.5%, 1.5%, and 1.9% greater than the experimental values for 1,1-, cis-, and trans-C_2H_2FCl, respectively.[40,41]

Upon ionization to form the cationic states, the noticeable changes in vibrational frequencies are as follows. Consider the cationic ground state first. For 1,1-$C_2H_2FCl^+$, ν_3 and ν_{11} decrease by 210 and 354 cm^{-1} (Table 4), respectively. Note that the order of ν_{11} (367 cm^{-1}) and ν_{12} (563 cm^{-1}) is reversed for the cation in comparison to the molecule (610 and 540 cm^{-1}, Table 4), which was discovered from the Duschinsky matrix elements and confirmed by visualizing the vibrational

Table 5. Harmonic Vibrational Frequencies (in cm^{-1}) of cis-C_2H_2FCl and Its Cations[a]

mode	X		X+	A+	
	B3LYP	expt[b]	B3LYP	B3LYP	TD-B3LYP
ν_1	3234	3114	3190	3024[c]	3128
ν_2	3203	3102	3171	3186	3202
ν_3	1707	1661	1554	1616	1683
ν_4	1353	1335	1393	1295	1327
ν_5	1254	1231	1316	1224	1253
ν_6	1068	1062	1125	1031	1077
ν_7	802	812	882	639	700
ν_8	653	656	683	570	596
ν_9	197	205	213	145	157
ν_{10}	897	857	933	918	926
ν_{11}	752	735	761	664	688
ν_{12}	457	442	317	417	433

[a]X stands for the neutral ground state, X+ for the cationic ground state, and A+ for the first excited state of cation. The calculation basis set is aug-cc-pVTZ. [b]Experimental values are taken from ref 41. [c]The underlines denote normal modes whose orders are changed in comparison to those of the ground state.

Table 6. Harmonic Vibrational Frequencies (in cm^{-1}) of trans-C_2H_2FCl and Its Cations[a]

mode	X		X+	A+	
	B3LYP	expt[b]	B3LYP	B3LYP	TD-B3LYP
ν_1	3223	3103	3177	2905	3062
ν_2	3217	3094	3173	3141	3204
ν_3	1696	1647	1559	1605	1664
ν_4	1323	1296	1304	1312	1338
ν_5	1240	1218	1288	1052	1153
ν_6	1128	1127	1255	1233	1250
ν_7	868	876	975	710	721
ν_8	447	447	464	428	427
ν_9	271	270	280	257	254
ν_{10}	922	888	832[c]	954	963
ν_{11}	822	784	928	689	723
ν_{12}	270	270	208	254	262

[a]X stands for the neutral ground state, X+ for the cationic ground state, and A+ for the first excited state of cation. The calculation basis set is aug-cc-pVTZ. [b]Experimental values are taken from ref 41. [c]The underlines denote normal modes whose orders are changed in comparison to those of the ground state.

modes with the GaussView (Revision 5.0.8, Gaussian, Inc.) software. For cis-$C_2H_2FCl^+$, ν_3 and ν_{12} decrease by 153 and 140 cm^{-1} (Table 5), respectively. For trans-$C_2H_2FCl^+$, while ν_3 decreases by 137 cm^{-1}, ν_6, ν_7, and ν_{11} increases by 127, 107, and 106 cm^{-1} (Table 4), respectively. The decrease in ν_3 for the three isomers can be attributed to the weakening of the C=C bond, a consequence of removing an electron from the C=C π orbital. For the first excited state of $C_2H_2FCl^+$, the vibrational frequencies reduce for most modes (Tables 4−6), which can be attributed to the ionization from the second-highest-occupied molecular orbital (SHOMO) with a′ symmetry, whose character is nonbonding for Cl and F atoms but is bonding for CH and CC.

Photoelectron Spectra. 1,1-C_2H_2FCl. Figure 2a shows the comparison between the simulated and experimental[24] photo-electron spectra of 1,1-$C_2H_2FCl^+(\tilde{X}^2A'')$. The simulated spectrum with fwhm = 180 cm^{-1} (Figure 2a_S2) is in harmony

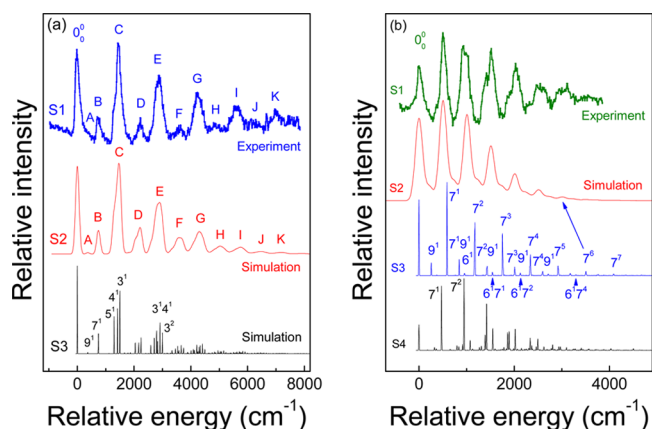**Figure 2.** (a) Experimental photoelectron spectrum (S1) of 1,1-$C_2H_2FCl^+(\tilde{X}^2A'')$ and B3LYP simulated spectrum with fwhm = 180 cm^{-1} (S2) and 10 cm^{-1} (S3). (b) Experimental photoelectron spectrum (S1) of 1,1-$C_2H_2FCl^+(\tilde{A}^2A')$, TD-B3LYP simulated spectrum with fwhm = 180 cm^{-1} (S2) and 10 cm^{-1} (S3), and B3LYP simulated spectrum with fwhm = 10 cm^{-1} (S4). In Figure 2b_S2, the vibrational frequencies were scaled by 0.86 (see text). The experimental threshold photoelectron spectra are taken from ref 24. (Reproduced with permission from the Institute of Physics. Copyright 2014.)

with the experimental spectrum (Figure 2a_S1) and depicts nearly one-to-one correspondence for bands A−K. However, Figure 2a_S3 with fwhm = 10 cm^{-1} clearly demonstrates that, except for bands A and B (9^1 and 7^1 transitions), each band consists of multiple transitions. In other words, the experimental resolution is not high enough to detect individual transitions. Moreover, the competing effects of different higher-order anharmonic contributions should also be identified carefully. Hence, it is hardly possible to determine precisely the vibrational frequencies and in particular the anharmonicity of the cation. The primary components of each band predicted by the present study are listed in the Supporting Information Table S7. It can be seen from Table S7 that band C contains the transitions of 5^1, 4^1, 7^2, and 3^1, with 3^1 most intensive (denoted by boldface). Thus, it might be safe to assign the maximum of band C to 3^1. However, the maximum of band E corresponds to 3^14^1 rather than 3^2 as Locht et al. assigned.[24] For bands F −I, each band maximum is a consequence of

overlap of several peaks, and it is inadequate to assign them to specific transitions.

The vibrational structure of photoelectron spectrum can be interpreted by inspecting geometrical changes between molecule and cation. In general, the larger the geometrical change, the likely the excitation of associated vibration. Upon ionization, R_{CC} lengthens by 8.45 pm, whereas R_{CF} and R_{CCl} shorten by 5.20 and 7.47 pm (Table 1), respectively. Meanwhile, A_{CCF} and A_{CCCl} decrease by 3.5° and 2.1°, respectively. Accordingly, the most active modes in the spectrum (Figure 2a_S3) are ν_3 (CC stretch), ν_4 (CH$_2$ scissor), ν_5 (CF stretch), and ν_7 (CCl stretch). The geometrical changes reflect the fact that the π orbital is bonding for C=C, but antibonding to the p orbitals of the Cl and F atoms.

Figure 2b depicts the comparison between the simulated and experimental[24] photoelectron spectra of 1,1-$C_2H_2FCl^+(\tilde{A}^2A')$. The spectral patterns predicted by the B3LYP and TD-B3LYP methods are distinct. For instance, the maximum-intensity band is 7^1 for TD-B3LYP (Figure 2b_S3), whereas it is 7^2 for B3LYP (Figure 2b_S4). On the other hand, the spectrum simulated by TD-B3LYP has a longer progression in ν_7 than by B3LYP. We found that the TD-B3LYP spectrum resembles the experimental spectrum better (Figure 2b). However, the TD-B3LYP method seems to overestimate the vibrational frequencies of 1,1-$C_2H_2FCl^+(\tilde{A}^2A')$. When the vibrational frequencies are scaled with a factor of 0.86 and they are taken into account for the FCF computation, the simulated spectrum (Figure 2b_S2) agrees well with the experiment (Figure 2b_S1). The scaling of vibrational frequencies alters the spectral pattern only slightly (Supporting Information Figure S1) because the spectral shape is governed primarily by geometrical changes. The most active vibrational modes are ν_7 (CCl stretch) and ν_9 (CFCl bend), corresponding to the greater change in R_{CCl} (10.00 pm) and A_{CCF} (8.5°) (Table 1). The primary geometrical changes stem from ionization of the SHOMO, which has a predominant contribution from the Cl atomic orbital.

Our assignments for the photoelectron spectrum of 1,1-$C_2H_2FCl^+(\tilde{A}^2A')$ are essentially in line with those reported by Locht et al. (Table 5 in ref 24). However, the peaks at 12.420, 12.482, and 12.592 eV, which are assigned by Locht et al. to 7^29^2, 7^39^2, and 7^59^2,[24] are suggested to reassign as 6^17^1, 6^17^2, and 6^17^4, respectively, according to Figure 2b_S3.

cis-C_2H_2FCl. The simulated photoelectron spectrum of *cis*-$C_2H_2FCl^+(\tilde{X}^2A'')$ is shown in Figure 3a, and the primary
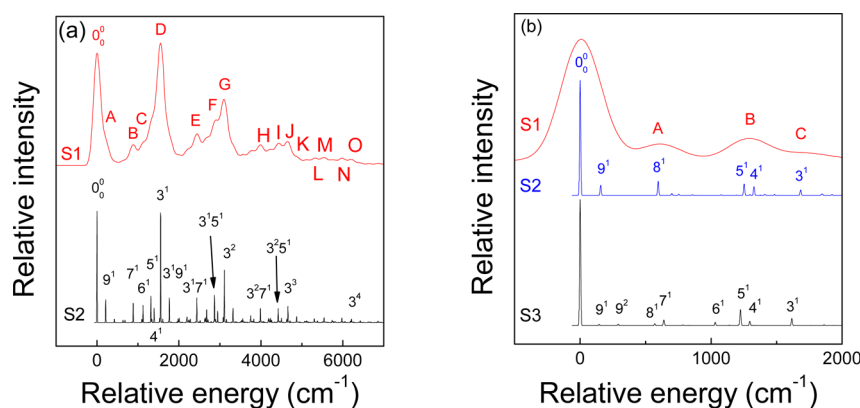

Figure 3. (a) B3LYP simulated photoelectron spectrum of *cis*-$C_2H_2FCl^+(\tilde{X}^2A'')$ with fwhm = 200 cm^{-1} (S1) and 10 cm^{-1} (S2). (b) TD-B3LYP simulated photoelectron spectrum of *cis*-$C_2H_2FCl^+(\tilde{A}^2A')$ with fwhm = 350 cm^{-1} (S1) and 10 cm^{-1} (S2) and B3LYP simulated spectrum with fwhm =10 cm^{-1} (S3).

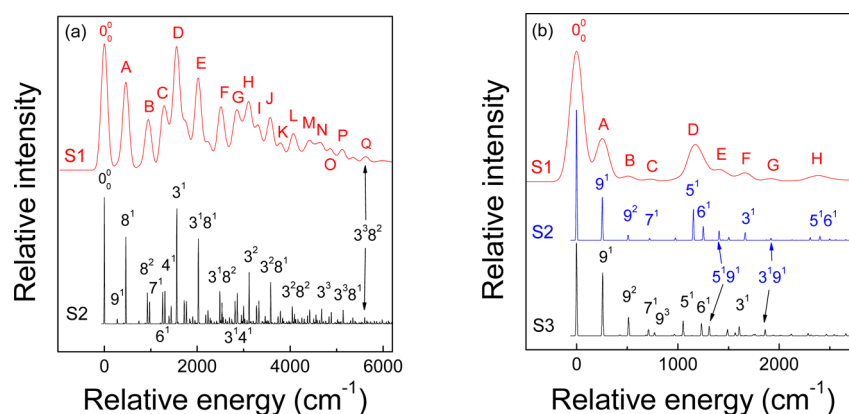**Figure 4.** (a) B3LYP simulated photoelectron spectrum of $trans$-$C_2H_2FCl^+(\tilde{X}^2A'')$ with fwhm = 160 cm^{-1} (S1) and 10 cm^{-1} (S2). (b) TD-B3LYP simulated photoelectron spectrum of $trans$-$C_2H_2FCl^+(\tilde{A}^2A')$ with fwhm = 150 cm^{-1} (S1) and 10 cm^{-1} (S2) and B3LYP simulated spectrum with fwhm =10 cm^{-1} (S3).

Table 7. Adiabatic Ionization Energies (AIEs) of C_2H_2FCl[a]

	1,1-C_2H_2FCl		cis-C_2H_2FCl		$trans$-C_2H_2FCl	
	X+	A+	X+	A+	X+	A+
AIE[b]	10.019	12.240	9.884	11.899	9.862	12.034
experiment[c]	10.02	12.24	9.87	11.87	9.88	12.05
experiment[d]	10.035	12.245	9.896	11.920	9.876	12.038

[a]X+ stands for the cationic ground state, and A+ for the first excited state of cation. [b]AIE by CCSD(T) CBS limit with B3LYP/aug-cc-pVTZ zero-point energy correction. [c]Reference 21. [d]References 24 and 25.

transitions are listed in Table S8. The simulated spectrum with fwhm = 200 cm^{-1} (Figure 3a_S1) is similar to the threshold photoelectron spectrum observed by Locht et al.,[25] except that the experimental intensities are stronger for bands B and H−O. The spectrum is mainly composed of the fundamental and combination bands ν_3–ν_7 and ν_9, in which ν_3 (CC stretch) is most prominent. It can be attributed to the ionization of an electron from the C=C π orbital, and the weakening of the π bond leads to the drastic change in R_{CC}, 7.74 pm (Table 2).

In our computation, the FCFs of ν_9 excited above v = 2 are negligible (Table S8), indicating that they could hardly be observed in the photoelectron spectrum. Nevertheless, Locht et al. assigned the progression of this mode as long as $8\nu_9$ (Table 3 of ref 25). We cannot rule out the possibility of their assignment, so we suggest that one can perform a higher-resolution photoelectron experiment to clarify which interpretation is more reasonable.

For cis-$C_2H_2FCl^+(\tilde{A}^2A')$, the simulated spectrum with fwhm = 350 cm^{-1} (Figure 3b_S1) is also in agreement with experiment. Band A corresponds to the 8^1 transition (CCl stretch). Band B is a consequence of the overlap of 5^1 (CH bend) and 4^1 (CH rock), whereas Locht et al. assigned it to 4^1.[25] Band C is due to 3^1 (CC stretch). Both B3LYP (Figure 3b_S3) and TD-B3LYP (Figure 3b_S2) give similar results, albeit the relative intensities are slightly different. The simple vibrational structure with the origin band the most intense results from ionization of the nonbonding in-plane Cl orbital. As a consequence, the equilibrium geometries undergo only minor changes upon ionization (Table 2).

$trans$-C_2H_2FCl. The simulated photoelectron spectrum of $trans$-C_2H_2FCl in the $\tilde{X}^2A''$ and $\tilde{A}^2A'$ states are shown in Figure 4a,b, respectively. The influence of Duschinsky effect on the spectrum is illustrated in Figure S2, where one can find that the intensity can be reduced (e.g., 8^2), enhanced (e.g., 6^1), or

unchanged (e.g., 4^1) due to different mixing of vibrational wave functions between two electronic states. Compared with experiment, the lower-resolution spectra (Figure 4a_S1 and Figure 4b_S1), together with those computed by EOM-CCSD (Figure S5), are all in harmony with experimental observations.[25] We list the active transitions with larger FCFs in Table S9. For the cationic ground-state $\tilde{X}^2A''$, ν_3 and ν_8 transitions are most active. Bands D, H, and N can be assigned to the progressions of ν_3 (3^1, 3^2, and 3^3), whereas bands A, E, J, and P are due to the 8^1, 3^18^1, 3^28^1, and 3^38^1 transitions (Figure 4a). For the first cationic state $\tilde{A}^2A'$, bands A, C, D, and F correspond to the fundamental transitions of 9^1, 7^1, 5^1, and 3^1, whereas other bands are due to overtones or combination bands (Figure 4b). The excitation of ν_6 up to four quanta, as Locht et al. reported (Table 7 in ref 25), is not supported by the present study.

Similar to cis-C_2H_2FCl, the $\tilde{X}^2A''$ and $\tilde{A}^2A'$ cationic states of $trans$-C_2H_2FCl are formed by removing an electron from the C=C π bonding orbital and the Cl nonbonding orbital, respectively. The nonbonding character of the latter leads to a simpler vibrational structure (Figure 4b) than the former (Figure 4a). For the $\tilde{X}^2A''$ state, the substantial changes in the bond lengths (+7.53, −6.61, and −8.42 for R_{CC}, R_{CF}, and R_{CCl}, respectively, Table 3) are due to ionization of the bonding orbital. On the contrary, the equilibrium structure deforms only slightly when the molecule is ionized from a nonbonding orbital to form the $\tilde{A}^2A'$ state.

Adiabatic Ionization Energy. The AIEs of the three isomers of C_2H_2FCl are listed in Table 7 and the CCSD energies are listed in Table S10. The values computed by the CBS limit method agree very well with the experimental ones. For 1,1-C_2H_2FCl ionized to the $\tilde{X}^2A''$ and $\tilde{A}^2A'$ states, the deviations are −0.016 and −0.005 eV when compared with threshold photoelectron experiment.[24] The corresponding

deviations are -0.012 and -0.021 eV for *cis*-C_2H_2FCl and -0.014 and -0.004 eV for *trans*-C_2H_2FCl.[25]

According to the results presented in the previous sections, we conclude that the simulated photoelectron spectra of 1,1-, *cis*-, and *trans*-C_2H_2FCl are in agreement with experiment in both ionization energies and intensity distributions. The vibrational structures are analyzed and the differences between previous experiments[24,25] and this work is discussed. We believe that without theoretical prediction of spectral patterns, the assignments of vibrational structures based on empirical or quantum-chemistry calculations are more difficult and less reliable and therefore should be regarded as tentative.

■ CONCLUSIONS

We have computed the equilibrium structures and harmonic vibrational frequencies of 1,1-, *cis*-, and *trans*-C_2H_2FCl (including the neutral ground state, the cationic ground state, and the first cationic state) by using the time-independent and time-dependent density-functional theory. Their photoelectron spectra were simulated from the Franck−Condon factors computed with the approach developed by our group. The adiabatic ionization energies were calculated by extrapolating the CCSD(T) energies to the CBS limit.

The simulated photoelectron spectra are generally in agreement with experiments and shed light on detailed insights. By comparing the simulated spectra of the three isomers of C_2H_2FCl with the threshold photoelectron electron experiments reported by Locht et al.,[24,25] we infer that the previous experimental resolutions are not capable of detecting individual transitions. Most experimental bands contain multiple transitions and it is inadequate to assign a band to a single vibrational excitation. Accordingly, the vibrational frequencies and anharmonicity coefficients reported by Locht et al.[24,25] need to be verified by advanced experiments with higher resolutions. In fact, Locht et al. assigned the spectra with the aid of high-level quantum-chemistry calculations (CCSD(FC), M06-2X, TD-DFT),[24,25] but this work shows that without the guide of theoretical intensity distributions, the spectral assignments based solely on the vibrational excitation energies would be more difficult and less reliable, because for polyatomic molecules many vibronic transitions might have similar excitation energies.

The adiabatic ionization energies computed by the CBS limit method are very accurate and the absolute deviations between theory and experiment range from 0.004 to 0.021 eV. The high-resolution photoelectron spectra of C_2H_2FCl are predicted and given in Tables S7−S9 for the reference of future experiments. Because both experimental and theoretical techniques of photoelectron spectroscopy are mature nowadays, we suggest that the agreement between experimental and theoretical spectra should be a key criterion to judge whether a spectral assignment is reasonable.

■ APPENDIX

Our formulas of Euler transformations are derived as follows. Suppose that a rotation matrix $\mathbf{R}$ transforms the atomic coordinates to new positions,

$$\mathbf{R}\begin{pmatrix} x \\ y \\ z \end{pmatrix} = \begin{pmatrix} x' \\ y' \\ z' \end{pmatrix} \tag{A1}$$

For rotations around the x, y and z-axes by angles α, β and γ, respectively, the $\mathbf{R}$ matrix is given by

$$\mathbf{R} = \begin{pmatrix} \cos\gamma & -\sin\gamma & 0 \\ \sin\gamma & \cos\gamma & 0 \\ 0 & 0 & 1 \end{pmatrix} \begin{pmatrix} \cos\beta & 0 & \sin\beta \\ 0 & 1 & 0 \\ -\sin\beta & 0 & \cos\beta \end{pmatrix} \begin{pmatrix} 1 & 0 & 0 \\ 0 & \cos\alpha & -\sin\alpha \\ 0 & \sin\alpha & \cos\alpha \end{pmatrix}$$

$$= \begin{pmatrix} c_2c_3 & s_1s_2c_3 - c_1s_3 & c_1s_2c_3 + s_1s_3 \\ c_2s_3 & s_1s_2s_3 + c_1c_3 & c_1s_2s_3 - s_1c_3 \\ -s_2 & s_1c_2 & c_1c_2 \end{pmatrix} \tag{A2}$$

where s denotes sine and c cosine functions, and subscripts 1, 2, and 3 stand for the rotation about the x, y, and z axes, respectively. To eliminate the rotation between two structures of a molecule, one needs to minimize the following quantity,

$$Q = \sum m[(x' - x_0)^2 + (y' - y_0)^2 + (z' - z_0)^2] \tag{A3}$$

where the sum goes over all atoms and the indices are omitted for clarity. The minimum of Q occurs at the structure where

$$\frac{\partial Q}{\partial \alpha} = 0, \qquad \frac{\partial Q}{\partial \beta} = 0, \qquad \frac{\partial Q}{\partial \gamma} = 0 \tag{A4}$$

Inserting eq A2 into eq A1, one has

$$x' = (c_2c_3)x + (s_1s_2c_3 - c_1s_3)y + (c_1s_2c_3 + s_1s_3)z$$
$$y' = (c_2s_3)x + (s_1s_2s_3 + c_1c_3)y + (c_1s_2s_3 - s_1c_3)z$$
$$z' = (-s_2)x + (s_1c_2)y + (c_1c_2)z \tag{A5}$$

By partial differentiating, one obtains

$$\frac{\partial x'}{\partial \alpha} = (c_1s_2c_3 - s_1s_3)y + (-s_1s_2c_3 + c_1s_3)z = s_2y' + c_2s_3z'$$
$$\frac{\partial y'}{\partial \alpha} = (c_1s_2s_3 - s_1c_3)y + (-s_1s_2s_3 - c_1c_3)z = -s_2x' - c_2c_3z'$$
$$\frac{\partial z'}{\partial \alpha} = (c_1c_2)y - (s_1c_2)z = c_2c_3y' - c_2s_3x' \tag{A6}$$

$$\frac{\partial x'}{\partial \beta} = (-s_2c_3)x + (s_1c_2c_3)y + (c_1c_2c_3)z = c_3z'$$
$$\frac{\partial y'}{\partial \beta} = (-s_2s_3)x + (s_1c_2s_3)y + (c_1c_2s_3)z = s_3z'$$
$$\frac{\partial z'}{\partial \beta} = (-c_2)x + (-s_1s_2)y + (-c_1s_2)z = -c_3x' - s_3y' \tag{A7}$$

$$\frac{\partial x'}{\partial \gamma} = (-c_2s_3)x + (-s_1s_2s_3 - c_1c_3)y + (-c_1s_2s_3 + s_1c_3)z = -y'$$
$$\frac{\partial y'}{\partial \gamma} = (c_2c_3)x + (s_1s_2c_3 - c_1s_3)y + (c_1s_2c_3 + s_1s_3)z = -x'$$
$$\frac{\partial z'}{\partial \gamma} = 0 \tag{A8}$$

Combining eqs A3 and A4, one gets

$$\frac{\partial Q}{\partial \alpha} = 2 \sum m \left[(x' - x_0) \frac{\partial x'}{\partial \alpha} + (y' - y_0) \frac{\partial y'}{\partial \alpha} + (z' - z_0) \frac{\partial z'}{\partial \alpha} \right] = 0$$

$$\frac{\partial Q}{\partial \beta} = 2 \sum m \left[(x' - x_0) \frac{\partial x'}{\partial \beta} + (y' - y_0) \frac{\partial y'}{\partial \beta} + (z' - z_0) \frac{\partial z'}{\partial \beta} \right] = 0$$

$$\frac{\partial Q}{\partial \gamma} = 2 \sum M \left[(x' - x_0) \frac{\partial x'}{\partial \gamma} + (y' - y_0) \frac{\partial y'}{\partial \gamma} + (z' - z_0) \frac{\partial z'}{\partial \gamma} \right] = 0$$

$$(A9)$$

Inserting eqs A6–A8 into eq A9, one has the following set of equations,

$$\sum m(x_0 y' - y_0 x') = 0$$

$$\left[\sum m(-x_0 z' + z_0 x') \right] c_3 + \left[\sum m(-y_0 z' + z_0 y') \right] s_3 = 0$$

$$\left[\sum m(-x_0 y' + y_0 x') \right] s_2 + \left[\sum m(-x_0 z' + z_0 x') \right] c_2 s_3$$
$$\quad + \left[\sum m(y_0 z' - z_0 y') \right] c_2 c_3 = 0$$

$$(A10)$$

For eq A10 to be valid, it can be shown that

$$\sum m(x_0 y' - y_0 x') = 0$$

$$\sum m(y_0 z' - z_0 y') = 0$$

$$\sum m(z_0 x' - x_0 z') = 0$$

$$(A11)$$

which is the so-called Eckart conditions. To find the desired trigonometric functions, we let all cosine functions in eq A5 as unity and neglect the terms involving the product of two or three sine functions,

$$x' \approx x - s_3 y + s_2 z$$

$$y' \approx s_3 x + y - s_1 z$$

$$z' \approx -s_2 x + s_1 y + z$$

$$(A12)$$

The approximation is valid when the rotation angles are small, which should be so as Q approaches the minimum. Compared with Chen's approach,[39] in which nonlinear terms are omitted after inserting eqs A1–A3 into A4, our approximation is tighter because fewer terms are neglected. Now, inserting eq A12 into eq A11, one has

$$\left[\sum m(y_0 y + z_0 z) \right] s_1 + \left(-\sum m y_0 x \right) s_2 + \left(-\sum m z_0 x \right) s_3$$
$$\quad = \sum m(z_0 y - y_0 z)$$

$$\left(-\sum m x_0 y \right) s_1 + \left[\sum m(z_0 z + x_0 x) \right] s_2 + \left(-\sum m z_0 y \right) s_3$$
$$\quad = \sum m(x_0 z - z_0 x)$$

$$\left(-\sum m x_0 z \right) s_1 + \left(-\sum m y_0 z \right) s_2 + \left[\sum m(x_0 x + y_0 y) \right] s_3$$
$$\quad = \sum m(y_0 x - x_0 y)$$

$$(A13)$$

from which the sine functions can be solved. Then, the cosine functions are calculated by

$$c = \sqrt{1 - s^2}$$

$$(A14)$$

All the matrix elements of **R** are thus obtained and the structure can be transformed. The new positions are checked whether they satisfy the Eckart conditions within some predetermined precision (say 10^{-15} amu·Å^2 in eq A13); if

not, the transformation is iterated until reaching the desired precision.

ASSOCIATED CONTENT

ⓢ Supporting Information

AUTHOR INFORMATION

Corresponding Author
*Jia-Lin Chang. Telephone: +886-4-2218-3564. Fax: +886-4-2218-3560. E-mail: jlchang@mail.ntcu.edu.tw.

Notes
The authors declare no competing financial interest.

ACKNOWLEDGMENTS

REFERENCES

(1) Chang, J.-L. A New Formula to Calculate Franck-Condon Factors for Displaced and Distorted Harmonic Oscillators. *J. Mol. Spectrosc.* **2005**, *232*, 102–104.

(2) Chang, J.-L. A New Method to Calculate Franck-Condon Factors of Multidimensional Harmonic Oscillators Including the Duschinsky Effect. *J. Chem. Phys.* **2008**, *128*, 174111.

(3) Lee, C.-L.; Yang, S.-H.; Kuo, S.-Y.; Chang, J.-L. A General Formula of Two-Dimensional Franck-Condon Integral and the Photoelectron Spectroscopy of Sulfur Dioxide. *J. Mol. Spectrosc.* **2009**, *256*, 279–286.

(4) Chang, J.-L.; Huang, S.-T.; Chen, C.-C.; Yang, T.-T.; Hsiao, C.-C.; Lu, H.-Y.; Lee, C.-L. Theoretical Calculations of C_{2v} Excited States of SO_2^+. *Chem. Phys. Lett.* **2010**, *486*, 12–15.

(5) Chang, J.-L.; Huang, C.-H.; Chen, S.-C.; Yin, T.-H.; Chen, Y.-T. An Analytical Approach for Computing Franck-Condon Integrals of Harmonic Oscillators with Arbitrary Dimensions. *J. Comput. Chem.* **2013**, *34*, 757–765.

(6) Duschinsky, F. On the Interpretation of Electronic Spectra of Polyatomic Molecules. *Acta Physicochim. URSS* **1937**, *7*, 551–566.

(7) Mebel, A. M.; Hayashi, M.; Liang, K. K.; Lin, S. H. Ab Initio Calculations of Vibronic Spectra and Dynamics for Small Polyatomic Molecules: Role of Duschinsky Effect. *J. Phys. Chem. A* **1999**, *103*, 10674–10690.

(8) Kikuchi, H.; Kubo, M.; Watanabe, N.; Suzuki, H. Computational Method for Calculating Multidimensional Franck-Condon Factors: Based on Sharp-Rosenstock's Method. *J. Chem. Phys.* **2003**, *119*, 729–736.

(9) Santoro, F.; Improta, R.; Lami, A.; Bloino, J.; Barone, V. Effective Method for the Computation of Optical Spectra of Large Molecules at Finite Temperature Including the Duschinsky and Herzberg-Teller Effect: The Q_x Band of Porphyrin as a Case Study. *J. Chem. Phys.* **2008**, *128*, 224311.

(10) Bloino, J.; Viczysko, M.; Crescenzi, O.; Barone, V. Integrated Computational Approach to Vibrationally Resolved Electronic Spectra: Anisole as a Test Case. *J. Chem. Phys.* **2008**, *128*, 244105.

(11) Barone, V.; Bloino, J.; Biczysko, M.; Santoro, F. Fully Integrated Approach to Compute Vibrationally Resolved Optical Spectra: From Small Molecules to Macrosystems. *J. Chem. Theory Comput.* **2009**, *5*, 540−554.

(12) Peluso, A.; Borrelli, R.; Capobianco, A. Photoelectron Spectrum of Ammonia, a Test Case for the Calculation of Franck-Condon Factors in Molecules Undergoing Large Geometrical Displacements upon Photoionization. *J. Phys. Chem. A* **2009**, *113*, 14831−14837.

(13) Borrelli, R.; Capobianco, A.; Peluso, A. Generating Function Approach to the Calculation of Spectral Band Shapes of Free-Base Chlorin Including Duschinsky and Herzberg-Teller Effects. *J. Phys. Chem. A* **2012**, *116*, 9934−9940.

(14) Grimminger, R.; Clouthier, D. J.; Tarroni, R.; Wang, Z.; Sears, T. J. An Experimental and Theoretical Study of the Electronic Spectrum of HPS, a Second Row HNO Analog. *J. Chem. Phys.* **2013**, *139*, 174306.

(15) Mok, D. K. W.; Lee, E. P. F.; Chau, F.-t.; Dyke, J. M. Simulated Photodetachment Spectra of AlH_2^-. *J. Chem. Phys.* **2013**, *139*, 014301.

(16) Götze, J. P.; Karasulu, B.; Thiel, W. Computing UV/Vis Spectra from the Adiabatic and Vertical Franck-Condon Schemes with the Use of Cartesian and Internal Coordinates. *J. Chem. Phys.* **2013**, *139*, 234108.

(17) Atkinson, R.; Carter, W. P. L. Kinetics and Mechanisms of the Gas-Phase Reactions of Ozone with Organic Compounds under Atmospheric Conditions. *Chem. Rev.* **1984**, *84*, 437−470.

(18) Atkinson, R. Kinetics and Mechanisms of the Gas-Phase Reactions of the Hydroxyl Radical with Organic Compounds under Atmospheric Conditions. *Chem. Rev.* **1986**, *86*, 69−201.

(19) Lake, R. F.; Thompson, S. H. Photoelectron Spectra of Halogenated Ethylenes. *Proc. R. Soc. London, Ser. A* **1970**, *315*, 323−338.

(20) Potts, A. W.; Benson, J. M.; Novak, I.; Svensson, W. A. Electron Correlation Effects in the Valence Shell Photoelectron Spectra of Haloethenes. *Chem. Phys.* **1987**, *115*, 253−260.

(21) Tornow, G.; Locht, R.; Kaufel, R.; Baumgärtel, H.; Jochims, H. W. The Vacuum Ultraviolet Photoabsorption and Photoelectron Spectroscopy of Fluorochloroethenes. The 1,1-, Cis- and Trans-C_2H_2FCl. *Chem. Phys.* **1990**, *146*, 115−128.

(22) Locht, R.; Leyh, B.; Hottmann, K.; Baumgärtel, H. The Spectroscopy of Ethylene and Its Derivatives. C_2H_4 and the Three C_2H_2FCl Isomers. The Cis- and Threshold Photoelectron Spectra. *BESSY Jahresber.* **1999**, 150−152.

(23) Harvey, J.; Hemberger, P.; Bodi, A.; Tuckett, R. P. Vibrational and Electronic Excitations in Fluorinated Ethene Cations from the Ground up. *J. Chem. Phys.* **2013**, *138*, 124301.

(24) Locht, R.; Dehareng, D.; Leyh, B. The Threshold Photoelectron Spectrum of the Geminal Chloro-Fluoro-Ethene (1,1-C_2H_2FCl) Isomer. Experiment and Theory. *J. Phys. B: At., Mol. Opt. Phys.* **2014**, *47*, 085101.

(25) Locht, R.; Dehareng, D.; Leyh, B. The Threshold Photoelectron Spectroscopy of the Cis- And Trans-1-Chloro-2-Fluoro-Ethene Isomers: An Experimental and Quantum Chemical Study. *J. Phys. B: At., Mol. Opt. Phys.* **2014**, *47*, 175101.

(26) Dewar, M. J. S.; Rzepa, H. S. Ground States of Molecules. 53. MNDO Calculations for Molecules Containing Chlorine. *J. Comput. Chem.* **1983**, *4*, 158−169.

(27) Bach, R. D.; Wolber, G. J. Nucleophilic Substitution at Vinylic Carbon: The Importance of the HOMO-HOMO Interaction. *J. Am. Chem. Soc.* **1984**, *106*, 1401−1409.

(28) Gambi, A.; Cazzoli, G.; Dore, L.; Mazzavillani, A.; Puzzarini, C.; Palmieri, P.; Baldan, A. Theoretical Molecular Structure and Experimental Dipole Moment of Cis-1-Chloro-2-Fluoroethylene. *Phys. Chem. Chem. Phys.* **2000**, *2*, 1639−1643.

(29) Puzzarini, C.; Cazzoli, G.; Dore, L.; Gambi, A. Molecular Structure of Cis-1-Chloro-2-Fluoroethylene from Ab Initio Calcu-

lations and Microwave Spectroscopy. *Phys. Chem. Chem. Phys.* **2001**, *3*, 4189−4194.

(30) Puzzarini, C.; Cazzoli, G.; Gambi, A. An Ab Initio Study of Trans-1-Chloro-2-Fluoroethylene: Equilibrium Structure and Molecular Properties. *J. Chem. Phys.* **2003**, *118*, 2647−2656.

(31) Cazzoli, G.; Puzzarini, C.; Gambi, A. Trans-1-Chloro-2-Fluoroethylene: Microwave Spectra and Anharmonic Force Field. *J. Chem. Phys.* **2004**, *120*, 6495−6501.

(32) Gambi, A.; Valle, R. G. D. Local Mode and Normal Mode Models for Molecules with Two Non-Equivalent C−H Bonds. *Mol. Phys.* **2007**, *105*, 1779−1787.

(33) Locht, R.; Dehareng, D.; Leyh, B. Vibronic Valence and Rydberg Transitions in Geminal Chloro-Fluoro-Ethene (1,1-C_2H_2FCl): A Spectroscopic and Quantum Chemical Investigation. *Mol. Phys.* **2014**, *112*, 1520−1539.

(34) Eckart, C. Some Studies Concerning Rotating Axes and Polyatomic Molecules. *Phys. Rev.* **1935**, *47*, 552−558.

(35) Sayvetz, A. The Kinetic Energy of Polyatomic Molecules. *J. Chem. Phys.* **1939**, *7*, 383−389.

(36) Ehrenson, S. Analysis of Least Motion Paths for Molecular Deformations. *J. Am. Chem. Soc.* **1974**, *96*, 3778−3784.

(37) Peterson, K. A.; Woon, D. E.; Dunning, T. H., Jr. Benchmark Calculations with Correlated Molecular Wave Functions. IV. The Classical Barrier Height of the H + H_2 → H_2 + H Reaction. *J. Chem. Phys.* **1994**, *100*, 7410−7415.

(38) Frisch, M. J.; Trucks, G. W.; Schlegel, H. B.; Scuseria, G. E.; Robb, M. A.; Cheeseman, J. R.; Scalmani, G.; Barone, V. B.; Mennucci, G. A.; Petersson, H.; et al. *Gaussian 09* (Revision A.02); Gaussian, Inc.: Wallingford, CT, 2009.

(39) Chen, Z. Rotation Procedure in Intrinsic Reaction Coordinate Calculations. *Theor. Chim. Acta* **1989**, *75*, 481−484.

(40) Leung, H. O.; Marshall, M. D.; Vasta, A. L.; Craig, N. C. Microwave Spectra of Eight Isotopic Modifications of 1-Chloro-1-Fluoroethylene. *J. Mol. Spectrosc.* **2009**, *253*, 116−121.

(41) Craig, N. C.; Lo, Y.-S.; Piper, L. G.; Wheeler, J. C. Vibrational Assignments and Potential Constants for Cis- and Trans-1-Chloro-2-Fluoroethylenes and their Deuterated Modifications. *J. Phys. Chem.* **1970**, *74*, 1712−1727.